

Supramolecular and electrical properties of ruthenium-based organometallic gels

Supplementary Information

Ilknur Hatice Eryilmaz, William Gallonde, Elsa Caytan, Olivier Jeannin, Franck Camerel, Stéphane Rigaut, Olivier Galangau, and Emanuele Orgiu

Table of Contents

Table of Contents.....	1
1. Synthesis and gel preparation	1
NMR spectra of Ru ₂	3
2. Electrochemical characterization	9
3. Electrical characterization of devices	9
4. FTIR & ATR-FTIR studies	13
5. Small-angle X-ray scattering (SAXS) characterization	16
7. References	18

1. Synthesis and gel preparation

Chemicals and solvents (HPLC, spectroscopic grade) were purchased from Merck-Sigma Aldrich, Acros Organics, Alfa Aesar, and Fisher Scientific and were used without any further treatment. Anhydrous (HPLC) solvents were obtained from a MBraun SPS-800 drying system. Dry triethylamine (NEt₃) was obtained after distillation on CaH₂. All reactions were carried out under an argon atmosphere using Schlenk techniques. Schlenk tubes were dried under vacuum using a heat gun.

1.1 Synthesis of Ru₁.

Ru₁ was synthesized by Galangau et al. according to a procedure described in a recent publication.¹

1.2 Synthesis of Ru₂.

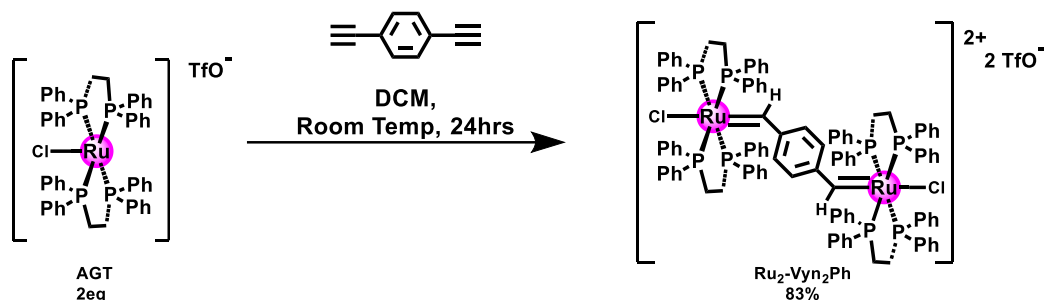
¹H, ¹³C, ³¹P spectra were recorded on a Bruker Avance III (400 MHz) and Bruker AMX-3300 (300 MHz) at 303 K. Relevant compounds were also characterized by 2D NMR using HSQC/HMQC, and HMBC sequences. Deuterated solvents were bought from Euriso-top. HR-MS spectra were obtained from the Centre Régional de Mesures Physiques de l'Ouest (CRMPO).

Syntheses of compounds Ru₂-Vyn₂Ph and Ru₂

Intermediate toluene bis-amide **(TBA)-PhA₁₂**¹, 1,4-Diethynylbenzene², **AGT**³ were synthesized according to procedures reported in the literature.

1. Compound **Ru₂-Vyn₂Ph**

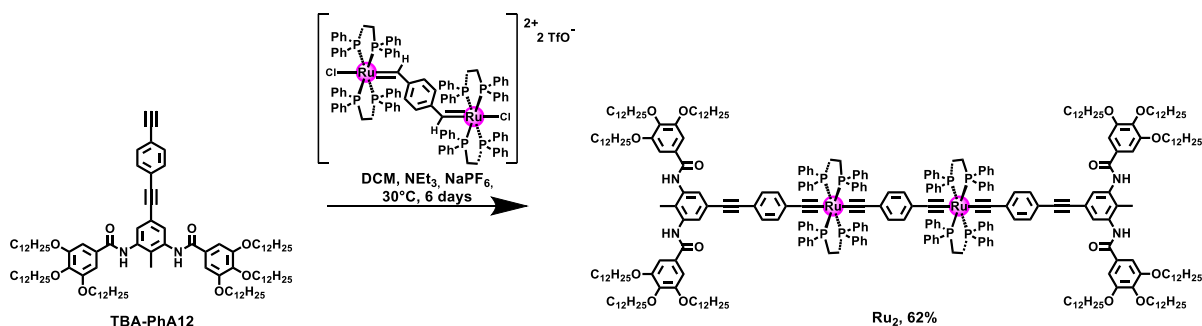
Intermediate **TBA-PhA₁₂**,¹ **1,4-Diethynylbenzene**,² **AGT**,³ were synthesized according to procedures reported in the literature.



A dried Schlenk tube equipped with a stirred bar was charged with **AGT** (0.432 g, 0.4 mmol, 2 eq.), **1,4-Diethynylbenzene** (0.025 g, 0.2 mmol, 1 eq.). Dry DCM (20 mL) was added *via* a syringe, the solution was stirred at room temperature for 24 hours. The precipitate was filtered by means of a canula and washed with cold DCM (3x 20mL), then dried under vacuum, to afford the desired compound as a green powder without further purification (m = 0.377 g, yield 83%).

³¹P NMR (121 MHz, CD₂Cl₂) δ 52.89.

2. Compound Ru₂



A dried Schlenk tube equipped with a stirred bar was charged with **Ru₂-Vyn₂Ph** (0.16 g, 0.07mmol, 1 eq.), **TBA-PhA₁₂** (0.23 g, 0.15 mmol, 2.1 eq.) and NaPF₆ (0.14 g, 0.85 mmol, 12 eq.). In a second Schleck, dry DCM (24 mL) and NEt₃ (0.69mL) were mixed & added to the reaction Schleck *via* canula, the solution was warmed to 30°C for 6 days. The reaction was monitored by ³¹P [¹H] (no lock procedure) NMR. The reaction was stopped by adding 80 mL of MeOH. The compound was filtered and dried under vacuum, to afford the desired product as yellow powder (m = 0.224 g, yield 62%).

¹H NMR (400 MHz, CD₂Cl₂) δ 7.92 (s, 4H), 7.66 (m, 20H), 7.43 (m, 16H), 7.31 – 7.14 (m, 28H), 7.05 (t, J = 7.6 Hz, 16H), 6.97 (t, J = 7.6 Hz, 16H), 6.71 (s, 4H), 6.67 (d, J = 7.9 Hz, 4H), 4.07 (t, J = 6.4 Hz, 16H), 4.03 (t, J = 6.6 Hz, 8H), 2.77 – 2.60 (m, 16H), 2.24 (s, 6H), 0.95 – 0.84 (m, 36H).

¹³C NMR (101 MHz, CD₂Cl₂) δ 166.19, 153.74, 141.90, 137.82, 137.52, 137.43, 137.33, 137.16, 134.85, 134.50, 131.29, 130.36, 129.78, 129.64, 129.09, 127.48, 126.05, 125.36, 122.75, 116.79, 106.16, 91.43, 88.89, 73.93, 69.81, 32.39, 32.37, 32.03, 31.91, 31.79, 30.81, 30.20, 30.16, 30.11, 30.05, 29.89, 29.87, 29.84, 29.81, 26.58, 23.13, 14.31, 13.54.

³¹P NMR (121 MHz, CD₂Cl₂) δ 52.97.

HRMS (ESI) m/z calculated for (C₃₂₀ H₄₃₀ N₄ O₁₆ P₈ ¹⁰²Ru₂) [M]³⁺: 1678.9642, found 1678.9669

NMR spectra of Ru₂

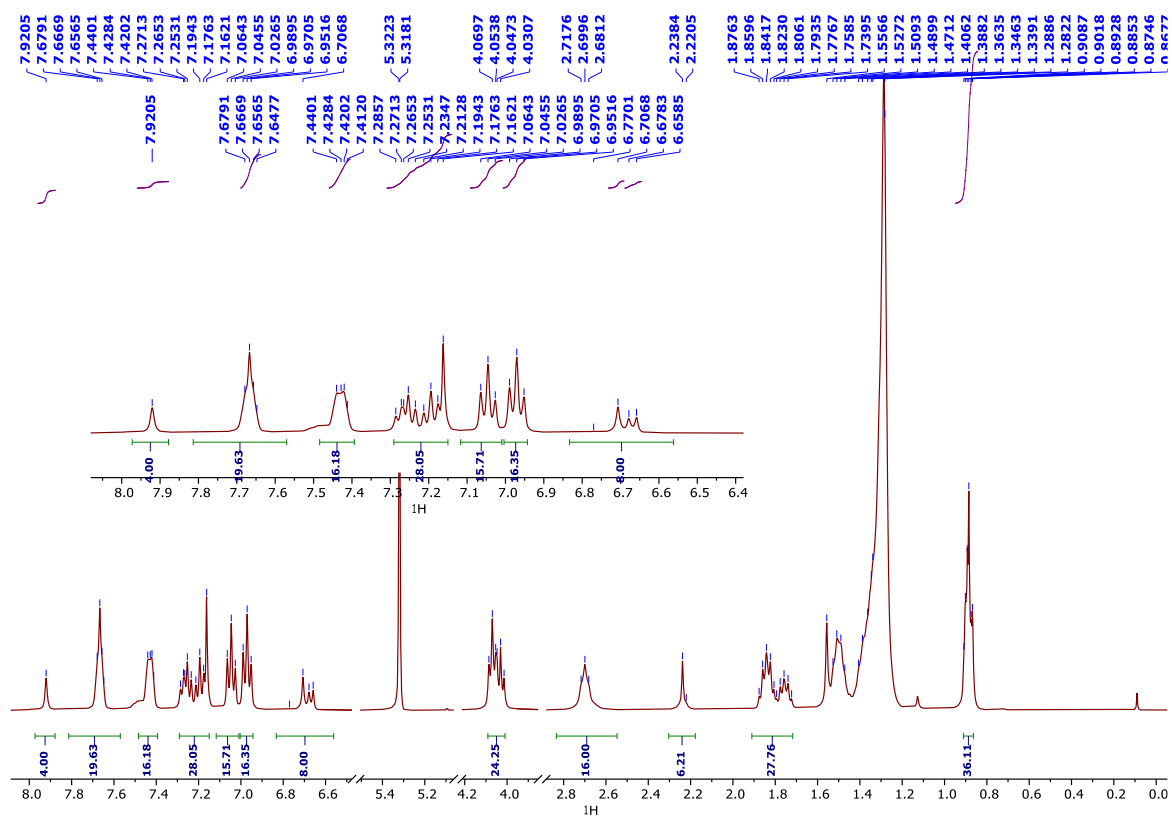


Figure S1 ¹H NMR Spectrum (CD₂Cl₂) of compound Ru₂

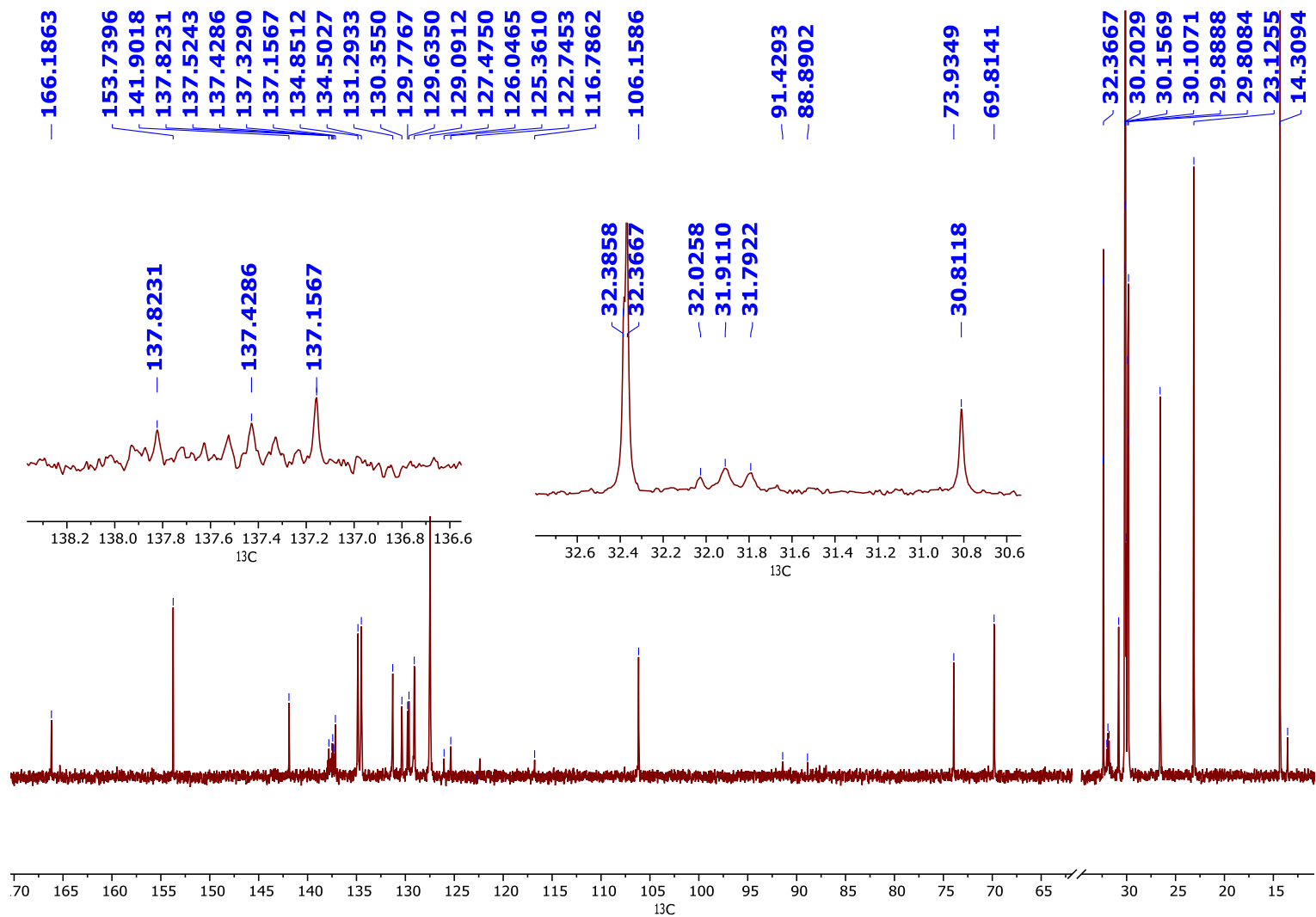


Figure S2 ^{13}C NMR spectrum (CD_2Cl_2) of compound Ru_2

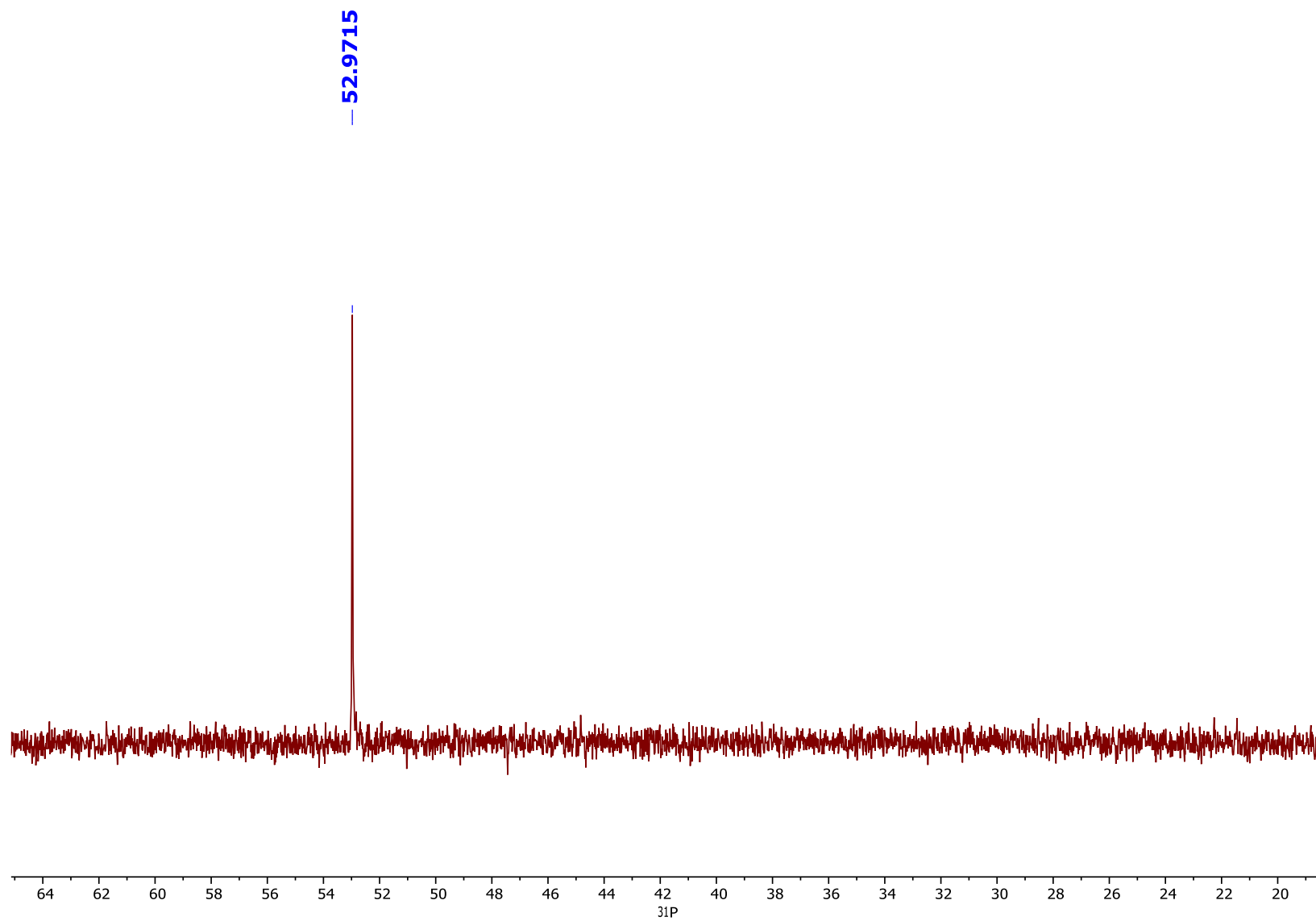


Figure S3 ^{31}P NMR spectrum (CD_2Cl_2) of compound Ru_2

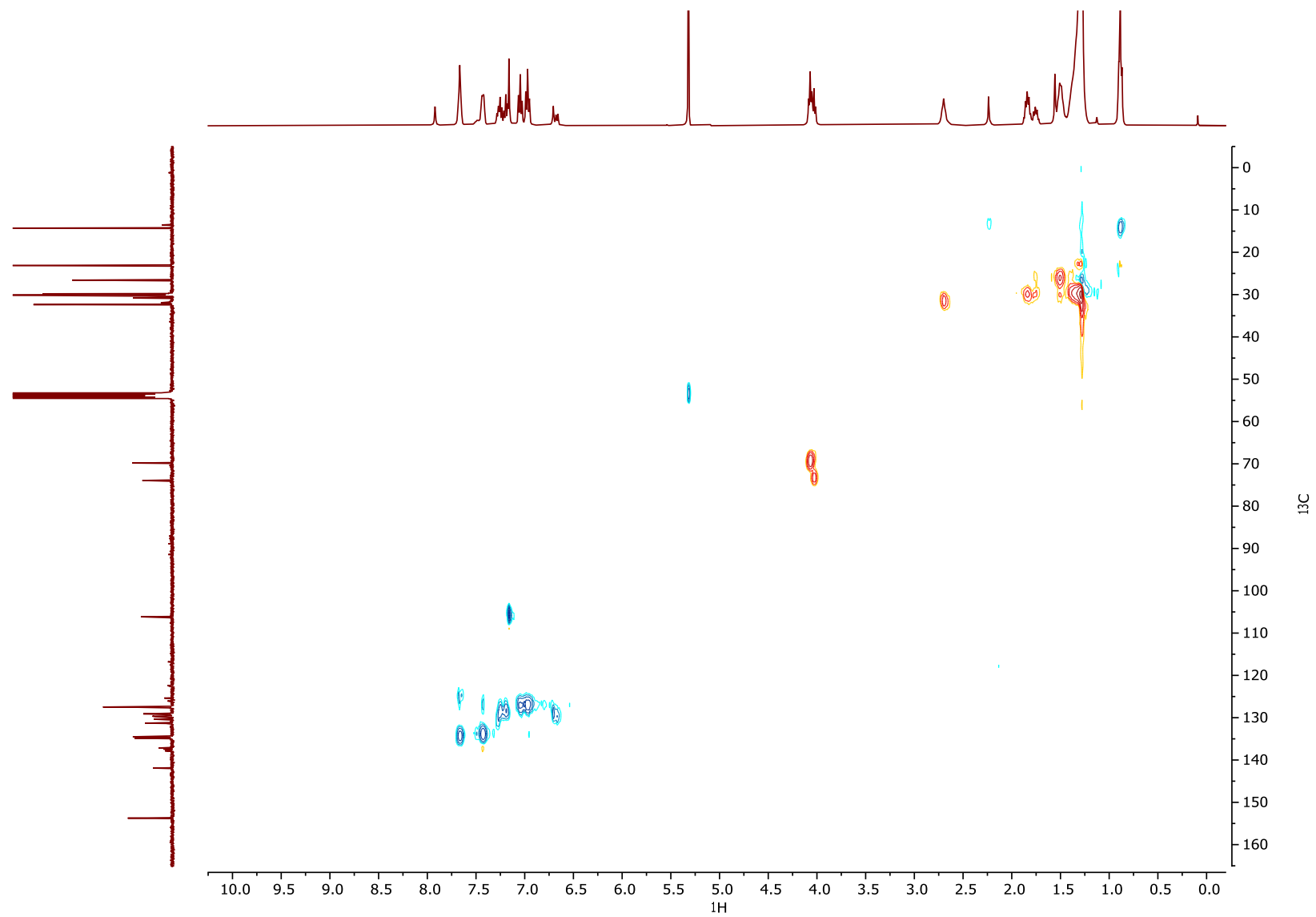


Figure S4 ^1H - ^{13}C HSQCed NMR experiment spectrum (CD_2Cl_2) of compound **Ru₂**

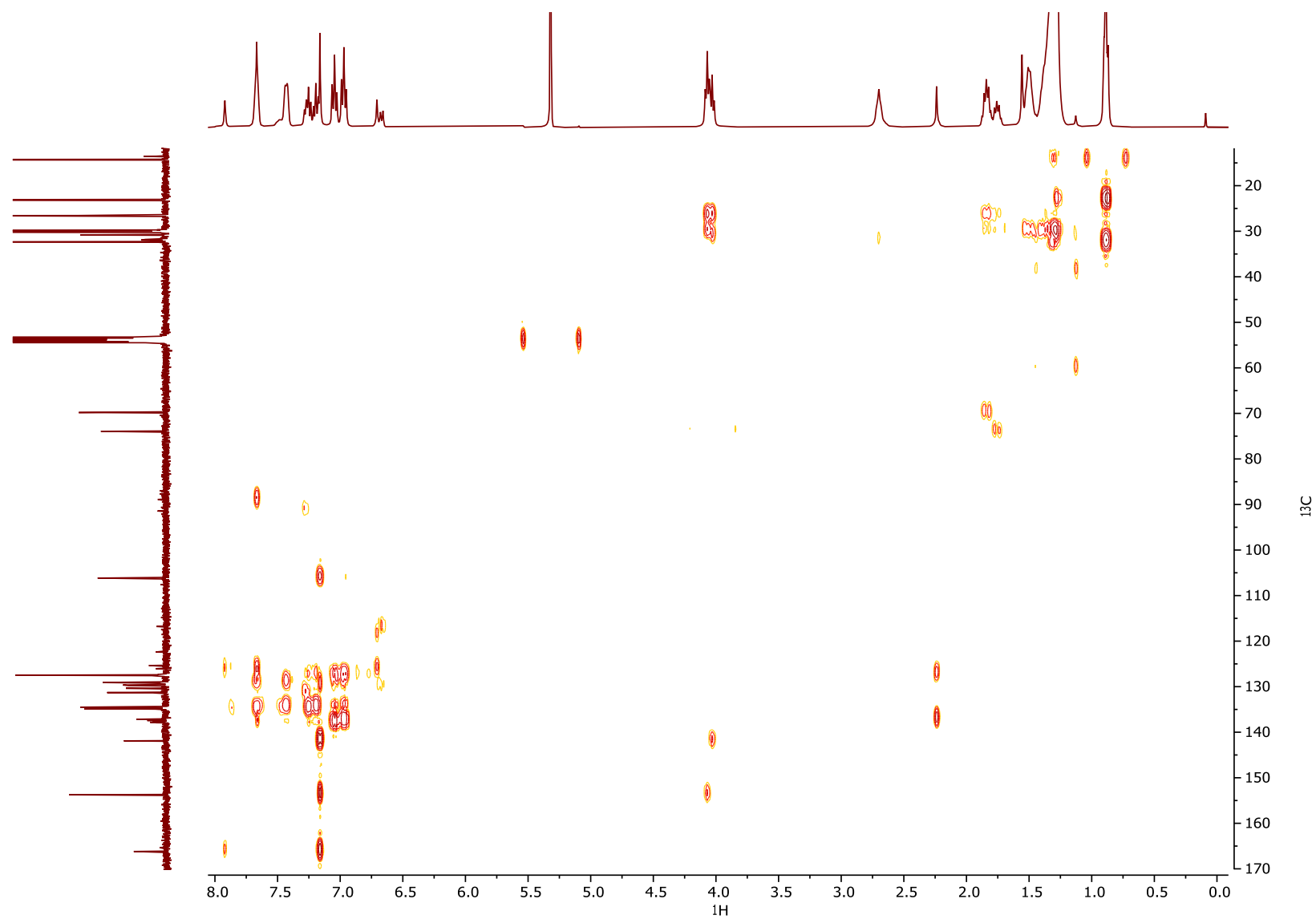


Figure S5 ^1H - ^{13}C HMBC NMR experiment spectrum (CD_2Cl_2) of compound **Ru₂**

1.3 Preparation of Ru₁ and Ru₂ gels

Ru₁ and Ru₂ (MW (Da) : 4017 and 5039, respectively) gels were prepared (20 and 50 mg/mL concentration, respectively) in toluene in a sealed glass vial and heated in the nitrogen filled glovebox. Gels were achieved through warming the solution at gelation temperature (T_{gel} : 24 °C) 60 °C and leaving for slow cooling under ambient temperature (21 °C) overnight. Subsequently vials were inverted to observe if a gel had formed. The observed gelation behaviors for Ru₁ are presented in a previous publication.¹ Yellow gel formation in toluene was observed and it was all stable at room temperature for several days depending on the gel amount. For the electrical characterization: Toluene 99.8%, dichloromethane (DCM) 99.8%, chloroform 99.9%, and chlorobenzene 99.9%, were purchased from Sigma-Aldrich and SiO₂/Si-n⁺⁺ substrates (thickness of SiO₂: 90 nm, and thickness of Si-n⁺⁺ 675 ± 20 μm) from Fraunhofer Institute for Photonic Microsystems IPMS, Dresden, Germany. To clean substrates, they were sonicated in acetone and isopropyl alcohol for 10 min respectively and dried with a nitrogen gun source and drain electrodes were used for 2-terminal devices. Chlorobenzene, chloroform, from Sigma-Aldrich.

1.4 Supramolecular polymerization as determined by VT-NMR

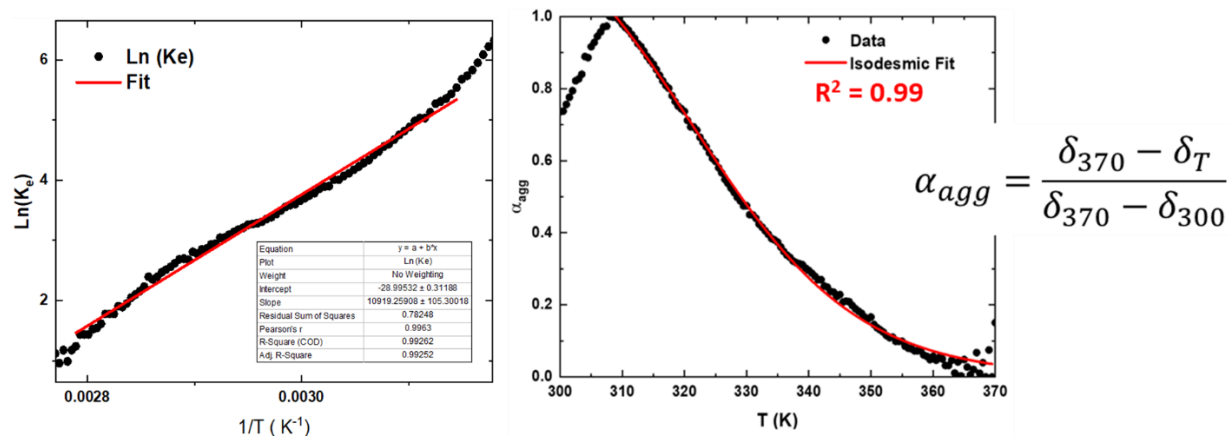


Figure S6 (Right) Aggregation parameter vs T plot showing excellent agreement with the isodesmic model. (Left) Pseudo Van't Hoff plot allowing for the determination of the growth enthalpy (entropy).

	C ₆ H ₆	toluene	<i>o</i> -xylene	<i>m</i> -xylene
Ru₁	G (7.5)	G (5)	G (7.5)	G (8)
Ru₂	G (14)	G (9)	G (9)	G (6)

Table S1: Supramolecular gelation of Ru₁ and Ru₂ (CGC in mM). G = Gel.

2. Electrochemical characterization

RedOx potentials & HOMO/LUMO levels of monometallic Ru₁ and bimetallic Ru₂ compounds.

	E _{ox} (vs SCE)		E ^{OX} _{onset} (vs SCE)	HOMO (eV) ^a	LUMO (eV) ^b
Monometallic (Ru ₁)	0.43 V	NA	0.42 V	-4.82	-2.02
Bimetallic (Ru ₂)	0.18 V	0.48 V	0.11 V	-4.51	-1.75

Table S2: ^aHOMO level were obtained from the cyclic-voltammetry measurements using the following relationship $\text{HOMO (eV)} = -[\text{E}^{\text{OX}}_{\text{onset}} + 4.4]$. ^bLUMO level was obtained from $\text{LUMO} = \text{HOMO} + \text{E}_{\text{HLB}}$ with E_{HLB} being the optical bandgap determined from spectrophotometric measurements. SCE stands for Saturated Calomel Electrode. NA = Not Applicable.

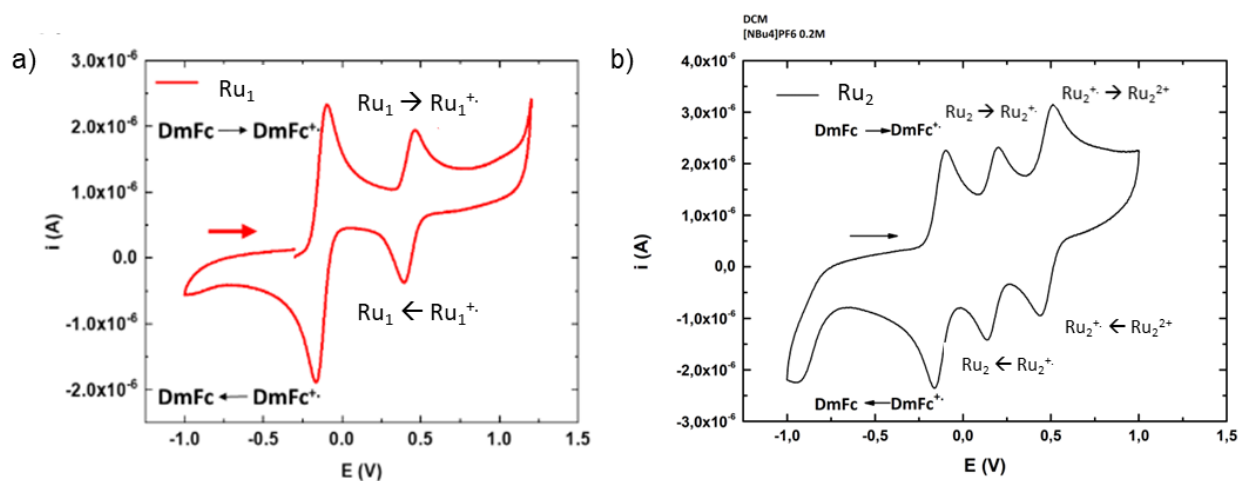


Figure S7 Cyclic voltammogram (V vs. SCE) of a) Ru₁ (in CH₂Cl₂, 0.2 M Tetrabutylammonium hexafluorophosphate)¹, b) Ru₂ (in CH₂Cl₂, 0.2 M Tetrabutylammonium hexafluorophosphate) [Note that DmFc stands for Decamethylferrocene].

3. Electrical characterization of devices

~3-4 μL of gel were dropped with Pasteur pipettes in the area between pre-patterned Au electrodes on SiO₂/Si-n⁺⁺ substrates for electrical characterization. Electrical characterization was performed in the glovebox (N₂) utilizing a Keithley 2636B source meter, interfaced by Kickstart™ software. I-V curves were recorded using two-terminal devices in a bottom-contact geometry starting from 15 V to -15 V regularly from pristine gel to dried state as well as rewetted forms. Transfer curves ($I_{\text{D}}-V_{\text{G}}$) were recorded by sweeping the gate voltage, V_{G} , from 15 V to -15 V at a constant V_{D} values at 0 V and -15 V.

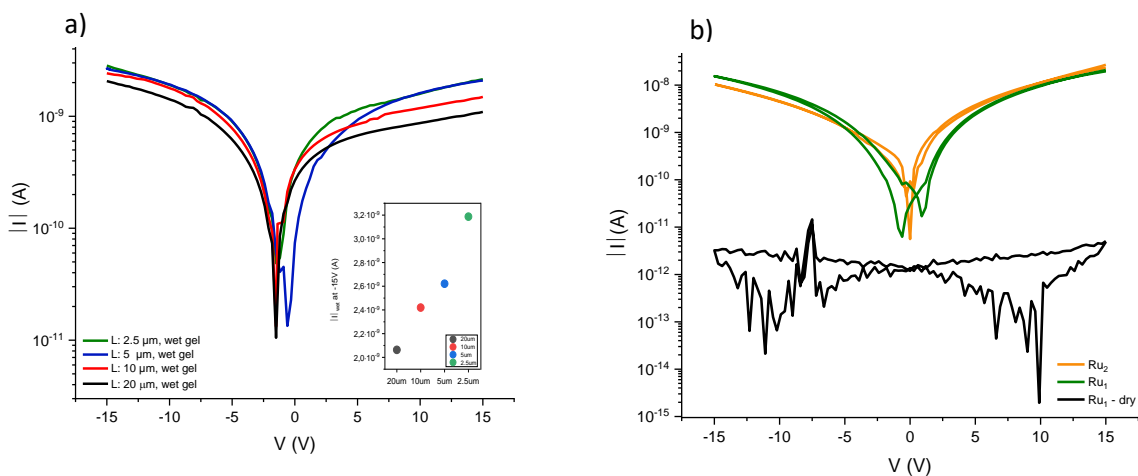


Figure S8 a) Channel length dependence of the current of pristine Ru₁-based gel (wet) prepared from toluene b) Comparative I-V curves, Ru₁ vs. Ru₂-based pristine gel properties.

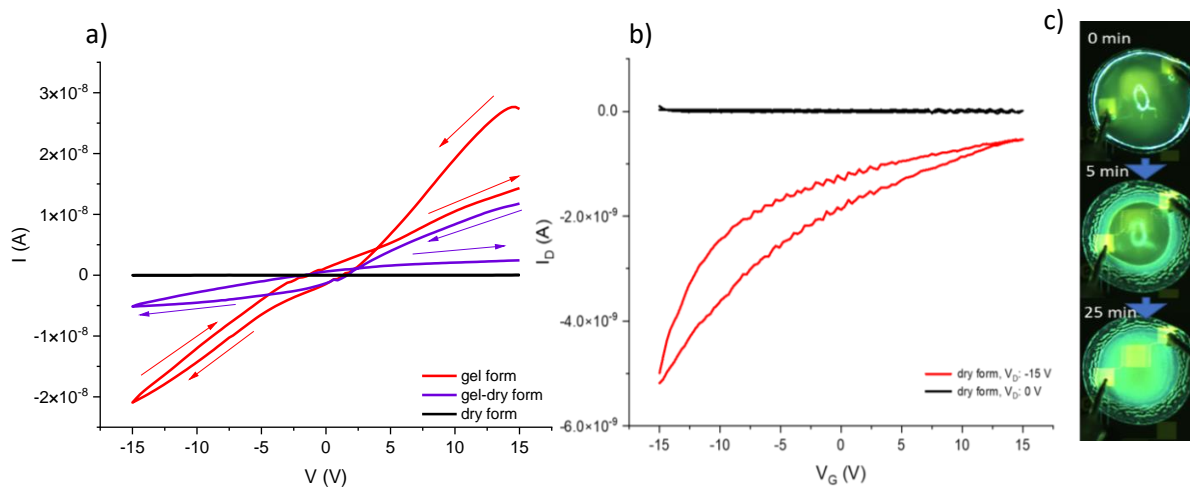


Figure S9 a) I-V characteristics during pristine Ru₁-based gel drying process (red: gel form, purple: drying gel, black: dried gel), b) transfer curves of pristine gel, c) microscope images of drying gel.

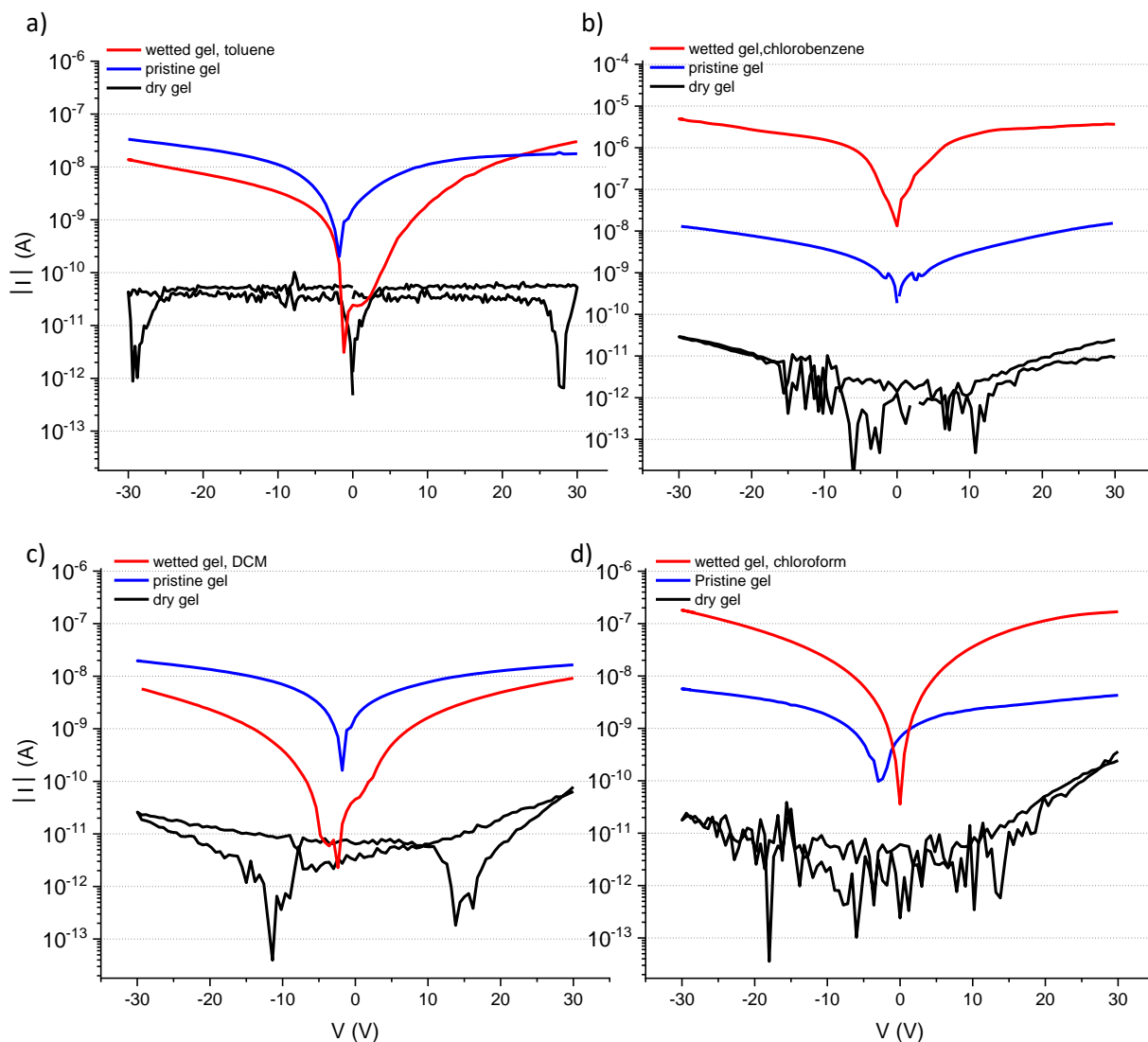


Figure S10 I-V curves of rewetted Ru₁-based dry gels with a) toluene, b) chlorobenzene, c) dichloromethane, d) chloroform. Pristine gel indicates the wet form of gel right after the initial deposition in between the electrodes.

DCM, I @ -30V (A)	Toluene, I @ -30V (A)	Chloroform, I @ -30V (A)	Chlorobenzene, I @ -30V (A)
6.05E-09	1,38E-08	9.04E-08	4.90E-06
5.62E-09	7,94E-09	4.34E-08	9.16E-07
	1,58E-08	2.65E-07	
Mean + σ	Mean + σ	Mean + σ	Mean + σ
(5.835 + 0.215)E-09	(1.25 + 0.33)E-08	(1.33+0.55)E-07	(2.9 +1.9)E-06

Table S3: Max current values at V = -30 V and their statistical variation, measured over 10 devices with Ru₁-based gels re-wetted with toluene, chlorobenzene, dichloromethane, chloroform.

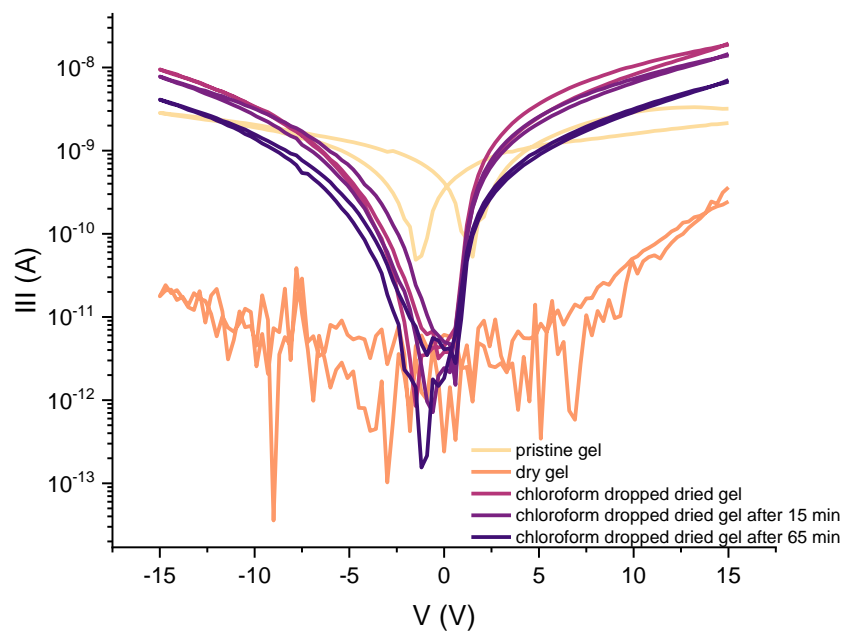


Figure S11 I-V curves of pristine Ru₁-based gel to rewetted gel (with chloroform) and its evolution by time.

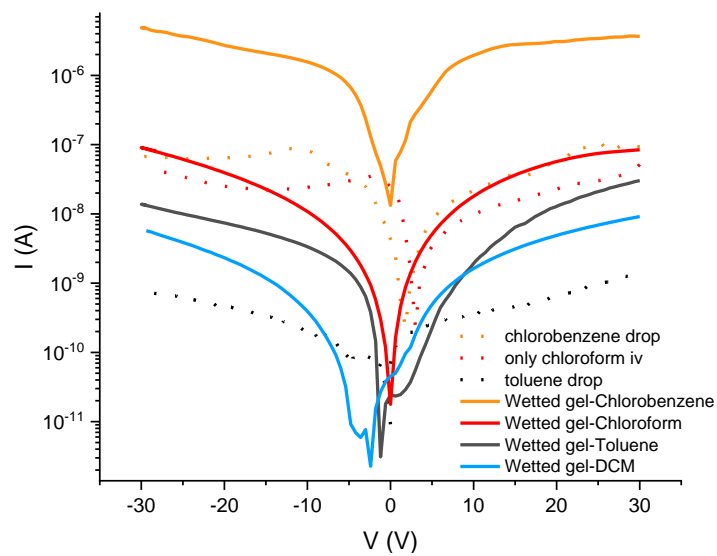


Figure S12 Summary of I-V curves of only solvents (dots) versus re-wetted Ru₁-based gels (lines).

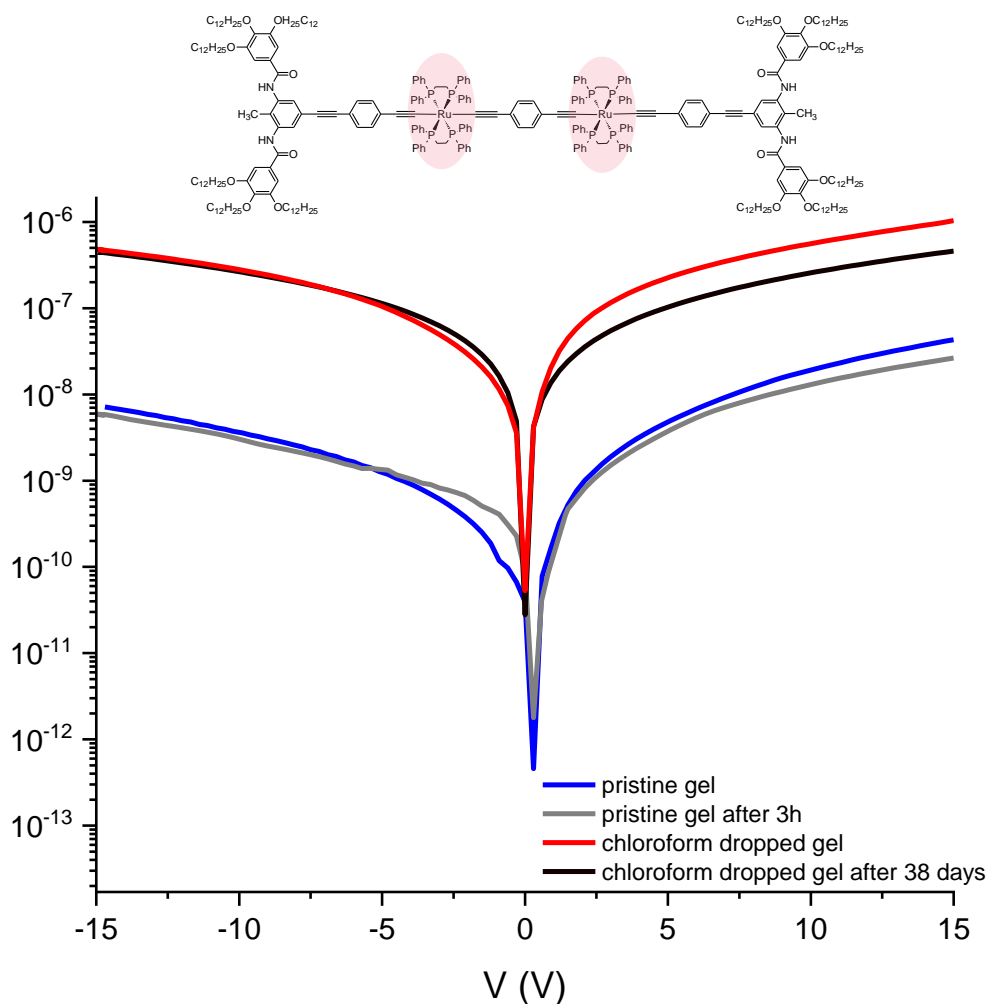


Figure S13 I-V curves of re-wetted (chloroform) Ru₂-based gel.

As previously indicated, slow-drying nature of Ru₂-based gel keeps its *wet* nature for long periods. However, we tested secondary solvent drop on drop casted gel after 3 hours when it was showing same as initial currents.

4. FTIR & ATR-FTIR studies

FTIR measurements were performed on a JASCO FTIR-4600 apparatus equipped with a PIKE Miracle ATR module featuring a diamond crystal, at a temperature of 20°C.

Prior to the experiments, background was recorded on air. Then, a known volume (V_{gel}) of the organometallic gel was dropped onto the ATR crystal and the acquisition was immediately started. We used

80 μL and 10 μL for the monometallic gel and the bimetallic gel, respectively. As the gel was allowed to slowly dry over time, FTIR spectra were recorded to monitor their time evolution. Dry state was reached when the FTIR spectrum no longer changed. It took almost 2h to the monometallic gel to reach the dry state when the bimetallic gel did not reach this dry state even after 2h.

Re-solvation experiments of the gels with toluene, chloro-benzene or chloroform were achieved by dropping the same V_{gel} volume. Spectra were acquired immediately after dropping the appropriate solvent volume. The time needed to acquire a spectrum was about 3 minutes.

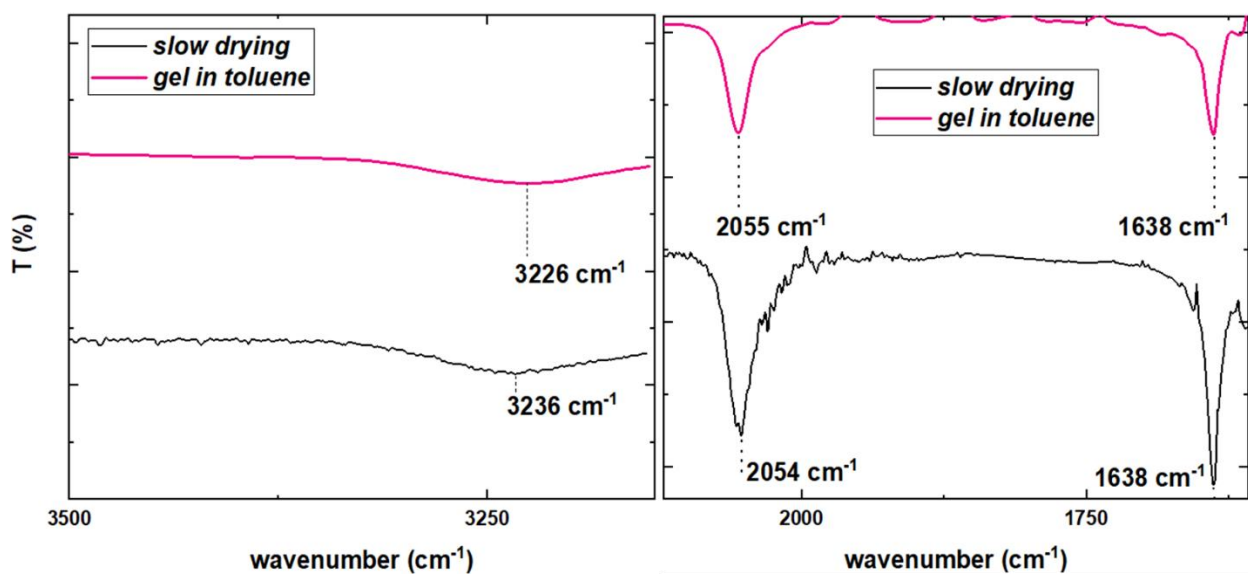


Figure S14 ATR-FTIR spectra of pristine wet gel, slow evaporated/xerogel and Ru_1 -based gel in toluene indicating hydrogen bonding weakening upon drying with blue shift of the N-H peak, with C-C, and C=O stretching bands almost independent from their drying method.

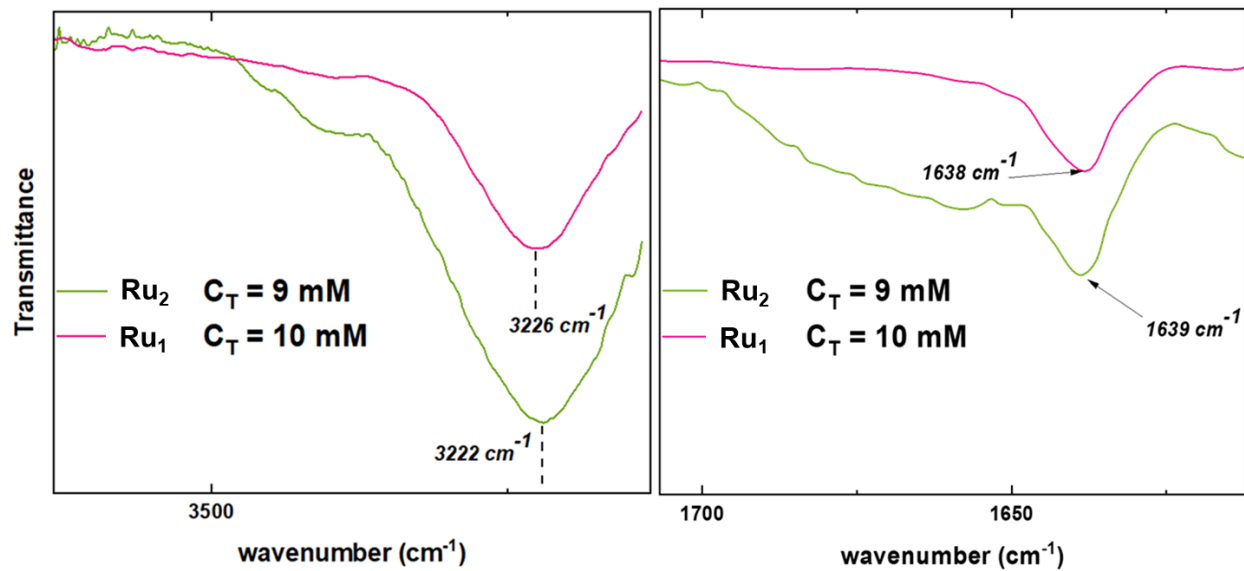


Figure S15 FTIR spectra of Ru₁ and Ru₂ gel states in toluene at room temperature. These data were acquired with FTIR operating in classical transmission mode. Spectrum resolution is 2 cm⁻¹.

5. Small-angle X-ray scattering (SAXS) characterization

SAXS characterization on Ru₁: Summary of the structure extracted by means of previous SAXS characterization [1] carried out on Ru₁:

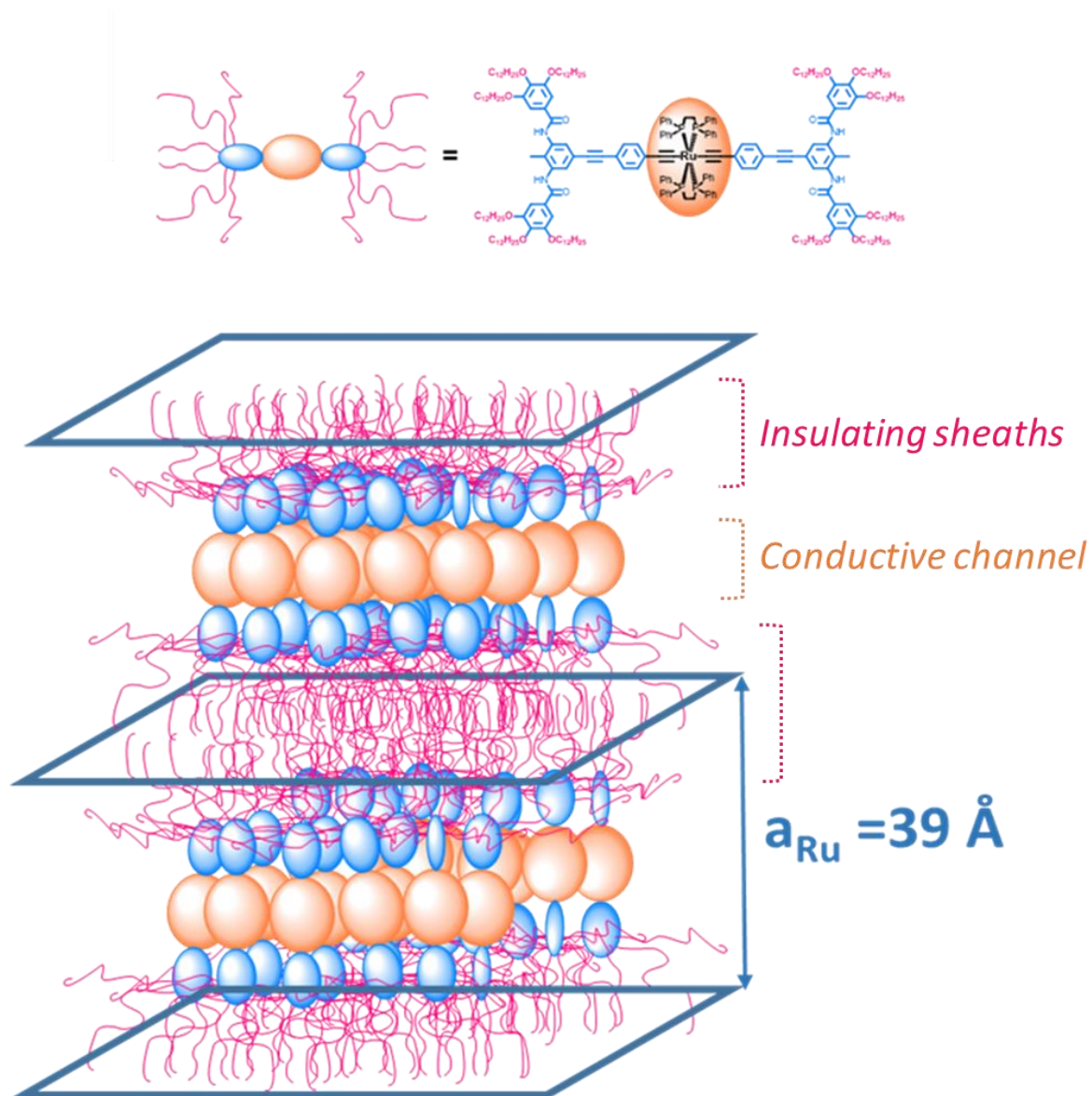


Figure S16 Molecular packing of Ru₁ in the gel as determined by SAXS [1]. The molecular alignment favors the creation of conductive channels encompassing the central organometallic centers, surrounded by insulating sheaths made of aliphatic chains.

SAXS characterization on Ru₂:

SAXS experiments were performed using a XENOCES GeniX3D low convergence copper micro source (50 W) ($\lambda = 1.541 \text{ \AA}$) equipped with FOX3D single reflection optics and point collimation. The patterns were collected with a Mar345 Image-Plate detector (Marresearch, Norderstedt, Germany). The samples were held in Lindeman glass capillaries (1.5 mm diameter). The capillaries were placed inside a Linkam HFX350-Capillary X-Ray stage which allow measurements from $-196 \text{ }^\circ\text{C}$ up to $350 \text{ }^\circ\text{C}$ with an accuracy of $0.1 \text{ }^\circ\text{C}$.

SAXS measurements (Figure S17) were first performed on a concentrated toluene gel ($C = 46 \text{ mg/mL}$). The diffraction patterns show an X-ray scattering intensity, I , that monotonously decreases with scattering vector modulus \mathbf{q} ($\mathbf{q} = (4\pi \sin \theta)/\lambda$, where 2θ is the scattering angle) as $I \propto \mathbf{q}^{-2}$ from 0.15 to 2.8 nm^{-1} . This scattering law is typical of two-dimensional planar objects, and its q -range shows that sheets have a thickness of $\sim 2.5 \text{ nm}$ and a considerable lateral spatial extension $> 42 \text{ nm}$. The observed oscillations are likely due to some inhomogeneity within the bidimensional objects. These experiments prove that the layers remain flat in suspension and do not wrinkle or fold.

The SAXS patterns also display two diffraction peaks at 1.23 and 0.94 nm in the wide angle region likely attributed to two-dimensional positional orders within the self-assembled layers. Observations of two dimensional objects is in accordance with the SEM pictures (section 6) revealing a layered structure.

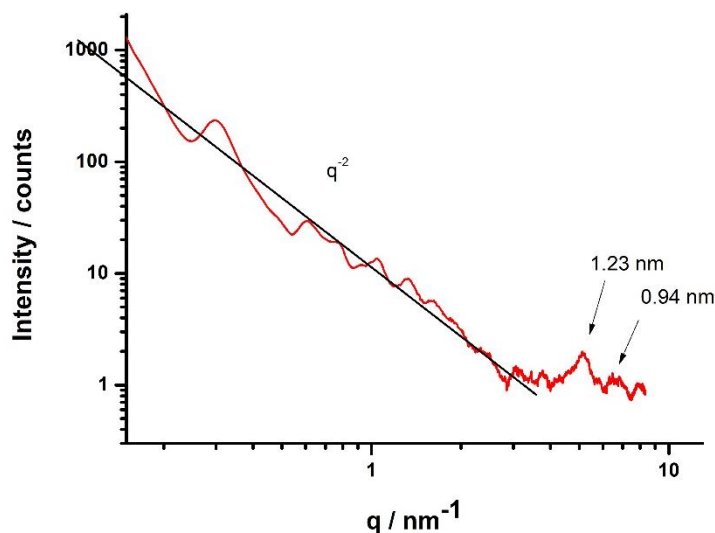


Figure S17 Scattered intensity I versus scattering vector modulus \mathbf{q} recorded on a toluene gel at 46 mg/mL (sample to detector distance = 842 mm).

6. Scanning Electron Microscopy (SEM) of Ru₂.

Scanning electron microscopy (SEM) images were acquired using a JEOL JSM-7100F with a SEI (secondary electron image) at a tension of 10 kV & a JEOL IT 300 LA with a SED (secondary electron detector) at a tension of 10 kV. The images were recorded at working distance fixed at 10.0 mm in high vacuum. SEM pictures were performed on a xerogel of Ru₂, prepared from a toluene gel (C = 46 mg/mL) by freeze drying.

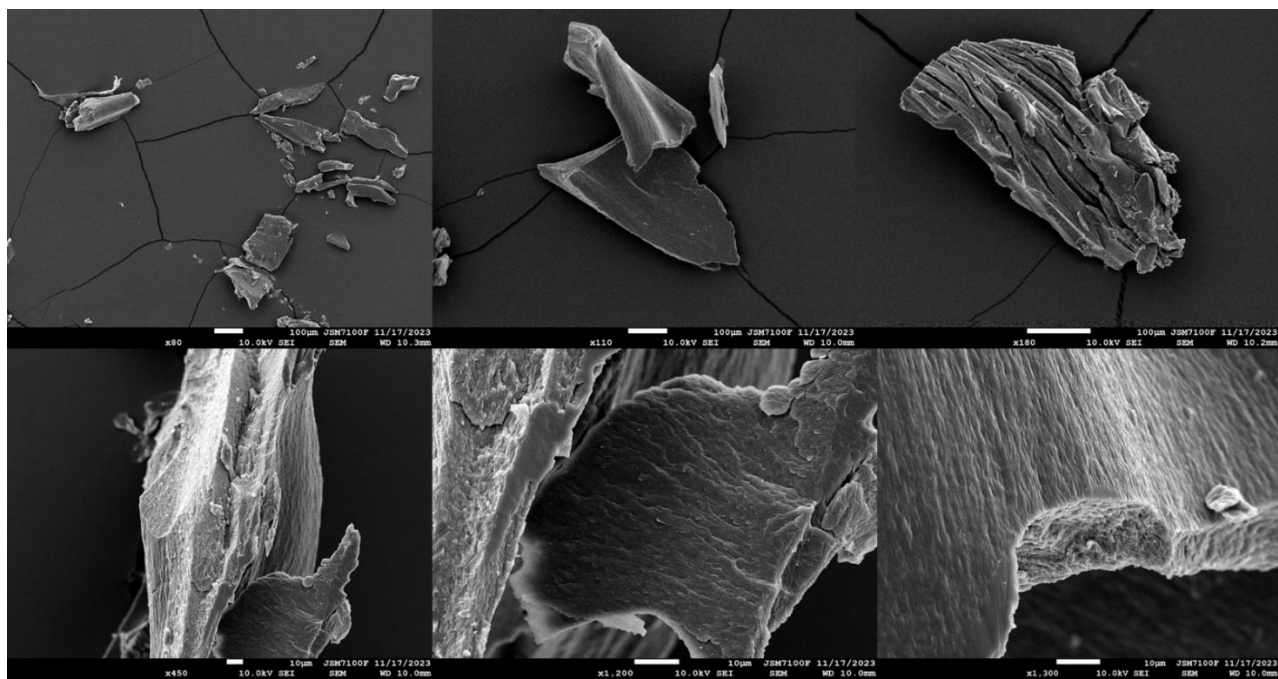


Figure S18. SEM pictures of Ru₂ xerogel showing the formation of bidimensional objects (nanosheets)

7. References

- (1) Galangau, O.; Daou, D.; El Beyrouti, N.; Caytan, E.; Mériadec, C.; Artzner, F.; Rigaut, S. *Inorg. Chem.* **2021**, *60* (15), 11474–11484.
- (2) Liu, K.; Wang, X.; Wang, F. *ACS Nano* **2008**, *2* (11), 2315–2323.
- (3) Fox, M. A.; Harris, J. E.; Heider, S.; Pérez-Gregorio, V.; Zakrzewska, M. E.; Farmer, J. D.; Yufit, D. S.; Howard, J. A. K.; Low, P. J. *J. Organomet. Chem.* **2009**, *694* (15), 2350–2358.